Chapter 16
Performance of Triple-Frequency High-Precision RTK Positioning with Compass

Hairong Guo, Jinlong Li, Junyi Xu, Haibo He and Aibing Wang

Abstract Compass is the first satellite navigation system providing the triple-frequency service in the world, and its triple-frequency carrier phase observations have obvious advantages on high-precision RTK positioning. In order to verify the success rate and reliability of Beidou triple frequency ambiguity resolution, the high-precision RTK positioning has been performed for Beidou/GPS observations by using geometry mode and geometry-free ambiguity resolutions. The results showed that, (1) By using geometry ambiguity resolutions, the success rate and reliability of ambiguity resolution for Beidou single-frequency, dual-frequency and triple-frequency RTK positioning is much better than that of GPS. (2) The accuracy of triple-frequency RTK positioning can reached centimeter level by using geometry-free ambiguity resolutions, and the method is not limited to baseline length. (3) When Beidou/GPS are combined, the position accuracy, success rate and reliability will be improved obviously, especially when the elevation angle is high or the signal is shielded.

Keywords Beidou · RTK · Triple-frequency carrier phase · Ambiguity resolution · Geometry mode · Geometry-free mode

H. Guo (✉) · H. He · A. Wang
Beijing Satellite Navigation Center, Beijing 100094, China
e-mail: hairongguo@263.net

J. Li · J. Xu
Institute of Surveying and Mapping, Information Engeering University, Zhengzhou 450052, China

J. Sun et al. (eds.), *China Satellite Navigation Conference (CSNC) 2013 Proceedings*, Lecture Notes in Electrical Engineering 243,
DOI: 10.1007/978-3-642-37398-5_16,

16.1 Introduction

The constellation of Compass satellite navigation system (first phase) consists of 14 satellites, including 5 GEO satellites, 5 IGSO satellites and 4 MEO satellites. The open service and authorized service will be provided at B1(1561.098 MHz), B2(1207.14 MHz) and B3(1268.52 MHz). The system will be full operated in 2012, and it shall be the first system which provides triple-frequency signals.

Centimeter-level RTK results can be achieved by using GNSS RTK technology which has already been widely applied in reference surveying, terrain surveying, cadastral surveying, GIS mapping and so on. One of the key problems for RTK positioning is the resolution of integer carrier ambiguity. Six or more satellites are needed for dual-frequency ambiguity resolution. In city areas, the number of visible satellites is fewer due to the shielding of high building. And then the applications of dual-frequency RTK positioning will be limited. However, fewer satellites are needed for triple-frequency ambiguity resolution. The integer ambiguity can be resolved successfully even when there are only four satellites. So the application scope of high-precision surveying will be extended with the triple-frequency RTK positioning technique.

The methods for the triple-frequency ambiguity resolution can generally be categorized in two kinds. The first kind is based on the geometry-free mode, such as TCAR and CIR. The other kind is based on geometry mode, such as the LAMBDA method. The successful rate of the two kinds is close for the short baselines [1–11]. The comparison of the dual-frequency and triple-frequency ambiguity resolution with the LAMBDA method shows that the triple-frequency carrier phase of Compass will have the big advantage in precision surveying.

16.2 Compass Triple-Frequency Ambiguity Resolution

16.2.1 Geometry Mode Based Ambiguity Resolution

For short baselines, the effect of satellite position errors, the ionosphere delay errors and troposphere delay errors is pretty small after the double-difference operation, the multi-path effect and the measurement errors, which is amplified by the difference operation, become the main error sources [1]. The triple-frequency double-difference observation equation can be expressed as,

$$\begin{aligned} \nabla\Delta P_i^j &= \nabla\Delta\rho + \nabla\Delta\varepsilon_{P_j^i} \\ \nabla\Delta\Phi^i{}_j &= \nabla\Delta\rho + \nabla\Delta N^i{}_j\lambda_j + \nabla\Delta\varepsilon_{\Phi_j^i} \end{aligned} \tag{16.1}$$

where,

The superscript i	Means the index of the satellite,
The subscript $j = 1, 2, 3$	Refers to the related carrier B_i,

P_j	Is the pseudo-range measurement of the carrier B_i (m),
Φ_j	Is the carrier phase measurement of the carrier B_i (m),
λ_j	Is the wavelength of the carrier of the carrier B_i (m),
N_j	Is the integer ambiguity of the carrier B_i (cycle),
ε_{P_j} and ε_{Φ_j}	Are the measurement noise of pseudo-range and carrier phase of the carrier B_i respectively (m)

After the linearization of the double-difference observation equation, the error equation can be written as,

$$v = (A_1\, A_2) \cdot \begin{pmatrix} X \\ a \end{pmatrix} - (\underbrace{L - f(X^0, a^0)}_{l}) \tag{16.2}$$

where,

v	Refers to the $(n-1)$ residual vector of the six kinds of double-difference measurements, n is the number of the satellites
X and X^0	Are the correction value and approximate value of position vector respectively
a and a^0	Are the correction value and approximate value of integer ambiguity vector respectively
A_1 and A_2	Are the sub-matrix of design matrix A with respect to the position parameters X and the integer ambiguity parameters a respectively
L	Is the observation vector
$f(\cdot)$	Means the function model of the observation L $l = L - f(X^0, a^0)$.

The target function is

$$\Omega = (l - A_1X - A_2a)^T P(l - A_1X - A_2a) = \min\, a \in Z^m\, X \in R^n \tag{16.3}$$

The normal equation can be written as

$$\begin{pmatrix} A_1^T PA_1 & A_1^T PA_2 \\ A_2^T PA_1 & A_2^T PA_2 \end{pmatrix} \cdot \begin{pmatrix} \widehat{X} \\ \widehat{a} \end{pmatrix} = \begin{pmatrix} A_1^T Pl \\ A_2^T Pl \end{pmatrix} \tag{16.4}$$

The above formula can be simplified as

$$\begin{pmatrix} N_{11} & N_{12} \\ N_{21} & N_{22} \end{pmatrix} \cdot \begin{pmatrix} \widehat{X} \\ \widehat{a} \end{pmatrix} = \begin{pmatrix} U_1 \\ U_2 \end{pmatrix} \tag{16.5}$$

where, P refers to the weight of the observations.

The value of X, a and their covariance matrix can be get,

$$\begin{aligned}
\widehat{a} &= (N_{22} - N_{21}N_{11}^{-1}N_{12})^{-1} \cdot (U_2 - N_{21}N_{11}^{-1}U_1) \\
\Sigma_{\widehat{a}} &= (N_{22} - N_{21}N_{11}^{-1}N_{12})^{-1} \\
\widehat{X} &= N_{11}^{-1}(U_1 - N_{12}\widehat{a}) \\
\Sigma_{\widehat{X}} &= N_{11}^{-1} + N_{11}^{-1}N_{12}\Sigma_{\widehat{a}}N_{21}N_{11}^{-1} \\
\Sigma_{\widehat{X}\widehat{a}} &= -N_{11}^{-1}N_{12}\Sigma_{\widehat{a}}
\end{aligned} \tag{16.6}$$

By using of the LAMBDA method [2, 4, 6, 10], the float point solution of the integer ambiguity $\widehat{a}$ is fixed as the integer $\breve{a}$

$$\Omega'' = (\widehat{a} - a)^T \Sigma_{\widehat{a}}^{-1}(\widehat{a} - a) = \min a \in Z^m \tag{16.7}$$

Substitute the integer ambiguity $\breve{a}$ back to (16.4) or (16.5), the ambiguity fixed solution of the position parameters $\breve{X}$ and their covariance can thus be calculated,

$$\breve{X} = N_{11}^{-1}(U_1 - N_{12}\breve{a}) = \widehat{X} + N_{11}^{-1}N_{12}(\widehat{a} - \breve{a}) = \widehat{X} - \Sigma_{\widehat{x}\widehat{a}}\Sigma_{\widehat{a}}(\widehat{a} - \breve{a}) \tag{16.8}$$

$$\Sigma_{\breve{X}} = N_{11}^{-1} = \Sigma_{\breve{X}} - \Sigma_{\breve{X}\hat{a}}\Sigma_{\widehat{a}}^{-1}\Sigma_{\widehat{a}\breve{X}} \tag{16.9}$$

16.2.2 Geometry-Free Mode Based Ambiguity Resolution

The geometry-free mode only uses the one way double difference measurement (including carrier phase and code phase measurement), and it's independent from the information of other satellite. This method is not influenced by the position of satellite, satellite clock error, ionosphere delay, troposphere delay and so on. It can resolve the ambiguity of medium and long baseline in a short time [5, 8, 12].

Step one: Calculate the ultra wide lane ambiguity directly by pseudorange.

The following equation is used to calculate the ambiguity:

$$\nabla\Delta N_{i,j,k} = \text{int}\left[\frac{\nabla\Delta\Phi_{i,j,k} - \nabla\Delta P_{l,m,n}}{\lambda_{i,j,k}} + \frac{\beta_{i,j,k} + \beta_{l,m,n}}{\lambda_{i,j,k}} \cdot \frac{\nabla\Delta K}{f_1^2} - \frac{\nabla\Delta\varepsilon_{\Phi_{i,j,k}} - \nabla\Delta\varepsilon_{P_{l,m,n}}}{\lambda_{i,j,k}}\right] \tag{16.10}$$

where, (i, j, k) and (l, m, n) are integer sets, int[•] means rounding, $\nabla\Delta$ refers to the double difference operator. To get reliable ambiguity, the influence of ionosphere delay and noise should be as small as possible. The following pseudo-range combination $P_{0,1,1}$ is used to resolve the ultrawide lane ambiguity

$$\nabla\Delta N_{0,-1,1} = \text{int}\left[\frac{\nabla\Delta\Phi_{0,-1,1} - \nabla\Delta P_{0,1,1}}{\lambda_{0,-1,1}} - \frac{\nabla\Delta\varepsilon_{\Phi_{0,-1,1}} - \nabla\Delta\varepsilon_{P_{0,1,1}}}{\lambda_{0,-1,1}}\right] \tag{16.11}$$

The above equation cancels the ionosphere delay. According to the error broadcast law, its variance can be expressed as

$$\sigma_{\left[\nabla\Delta N_{0,-1,1}\right]} = \sqrt{\frac{\sigma^2_{\nabla\Delta\Phi_{0,-1,1}} + \sigma^2_{\nabla\Delta P_{0,1,1}}}{\lambda^2_{0,-1,1}}} \tag{16.12}$$

Step two: Calculate the wide lane ambiguity $\nabla\Delta N_{1,0,-1}$ and $\nabla\Delta N_{1,-1,0}$ directly by pseudorange.

The principle is the same as step one, the wide lane ambiguity is calculated as:

$$\begin{aligned}\nabla\Delta N_{1,0,-1} &= \text{int}\left[\frac{\nabla\Delta\Phi_{1,0,-1} - \nabla\Delta P_{1,0,1}}{\lambda_{1,0,-1}} - \frac{\nabla\Delta\varepsilon_{\Phi_{1,0,-1}} - \nabla\Delta\varepsilon_{P_{1,0,1}}}{\lambda_{1,0,-1}}\right] \\ \nabla\Delta N_{1,-1,0} &= \text{int}\left[\frac{\nabla\Delta\Phi_{1,-1,0} - \nabla\Delta P_{1,1,0}}{\lambda_{1,-1,0}} - \frac{\nabla\Delta\varepsilon_{\Phi_{1,-1,0}} - \nabla\Delta\varepsilon_{P_{1,1,0}}}{\lambda_{1,-1,0}}\right]\end{aligned} \tag{16.13}$$

Step three: Calculate the ionosphere-free pseudorange and ionosphere delay by using two wide lane carrier phase measurement.

The ionosphere-free pseudorange is calculated as:

$$\begin{aligned}\nabla\Delta\Phi_{IFP} = &\frac{f_2}{f_2 - f_3}\left(\nabla\Delta\Phi_{1,-1,0} - \nabla\Delta N_{1,-1,0}\cdot\lambda_{1,-1,0}\right) \\ &- \frac{f_3}{f_2 - f_3}\left(\nabla\Delta\Phi_{1,0,-1} - \nabla\Delta N_{1,0,-1}\cdot\lambda_{1,0,-1}\right)\end{aligned} \tag{16.14}$$

The ionosphere delay is mitigated by Eq. (16.14), while the carrier noise is amplified, its variance is:

$$\sigma_{[\nabla\Delta\Phi_{IFP}]} \approx 27.3\sigma_{\Delta\nabla\varphi}(m) \tag{16.15}$$

The ionosphere delay is calculated as:

$$\frac{\nabla\Delta K}{f_1^2} = \frac{f_2 f_3}{f_1(f_2 - f_3)}\left[\left(\nabla\Delta\Phi_{1,0,-1} - \nabla\Delta N_{1,0,-1}\cdot\lambda_{1,0,-1}\right) - \left(\nabla\Delta\Phi_{1,-1,0} - \nabla\Delta N_{1,-1,0}\cdot\lambda_{1,-1,0}\right)\right] \tag{16.16}$$

its variance is:

$$\sigma_{\left[\frac{\nabla\Delta K}{f_1^2}\right]} \approx 21.4\sigma_{\Delta\nabla\varphi}(m) \tag{16.17}$$

Step four: Calculate the third linear independent ambiguity $\nabla\Delta N_1$ by using two wide lane carrier phase measurement.

Assume that the carrier phase measurement equation of the third linear independent ambiguity is:

$$\nabla\Delta\Phi_1 = \nabla\Delta\rho - \beta_1\cdot\frac{\nabla\Delta K}{f_1^2} + \nabla\Delta N_1\lambda_1 + \nabla\Delta\varepsilon_{\Phi,1} \tag{16.18}$$

Substituting the ionosphere-free pseudorange and ionosphere delay into Eq. (16.18), then

$$\nabla\Delta N_1 = \frac{\nabla\Delta\Phi_1 - \nabla\Delta\Phi_{IF}}{\lambda_1} + \frac{\beta_1}{\lambda_1}\cdot\frac{\nabla\Delta K}{f_1^2} + \varepsilon_{\nabla\Delta N_1} \tag{16.19}$$

It can be seen from Eq. (16.19) that $\nabla\Delta N_1$ is mainly influenced by the noise of carrier phase, and by averaging for a while, the reliable ambiguity can be acquired.

Step five: Calculate ambiguity $\nabla\Delta N_2$, $\nabla\Delta N_3$

16.3 Calculation and Analysis

16.3.1 Data

A test was performed in Beijing on December 19, 2012 by using two Beidou/GPS dual system receiver that produced by Sinan company. The receiver was located at two test stations whose accuracy position were already known. The baseline is about 4.2 m. The signal of Beidou B1/B2/B3 and GPS L1/L2 can be received by the receiver. The sampling interval is 1 s, the elevation is 10°, and the test lasted 1 day (Fig. 16.1).

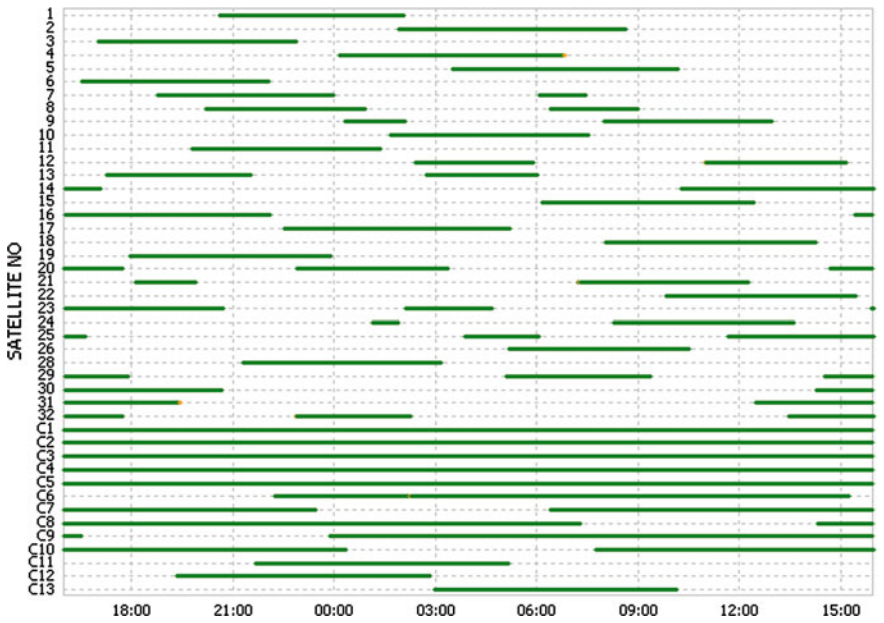

Fig. 16.1 BDS/GPS Satellite Visibility (elevation, 10)

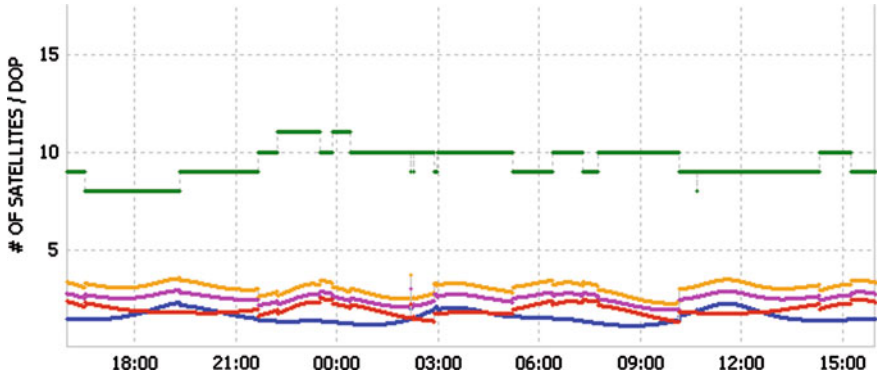

Fig. 16.2 DOP value and No. of BDS satellites (elevation, 10)

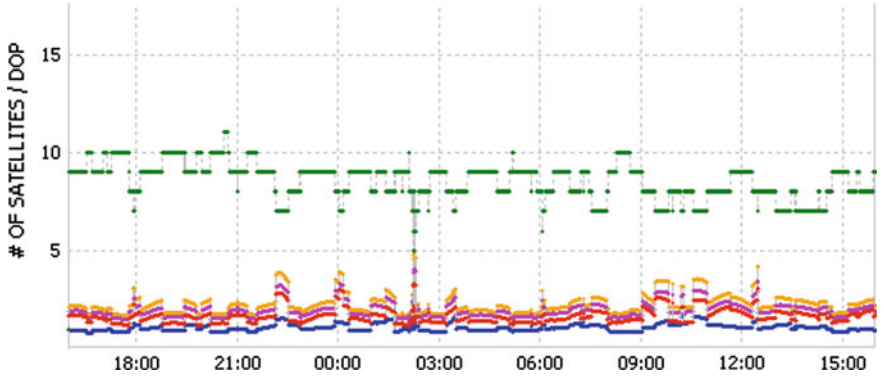

Fig. 16.3 DOP value and No. of GPS satellites (elevation, 10)

In Figs. 16.2 and 16.3, the top part of the figure depicts the number of the visible satellite, the bottom part of the figure depicts the value of DOP, from top to bottom they respectively represent GDOP, PDOP, VDOP and HDOP.

It can be seen from the above result that: (1) In Beijing area, the five GEO can be seen for all the day, the five IGSO can be seen for about 18 h, the four MEO can be seen for about 7 h. While for GPS, the average visible time of the satellite is about 6 h. (2) For Beidou, at least 8 satellite are visible, the number of visible satellite is about 9–10. While for GPS, the number of visible satellite is about 7–9, and sometimes only 5 satellite can be seen. (3) The DOP of GPS is a little better than that of Beidou, however, the DOP of Beidou varies more smoothly than that of GPS, and the DOP of GPS change frequently with the variation of the number of visible satellite.

16.3.2 Calculation and Analysis

The geometry mode and geometry-free mode are used for ambiguity resolution. The elevation is 10°. For geometry mode, the ration test is used for validation, and the threshold is 2.0. For geometry free mode, the threshold for rounding is 0.4. The epochs that pass the test is used for Fixed rate statistics, and the epochs that the three dimension error between fixed solution and the coordinate is smaller than 10 cm is used for success rate statistics.

It can be seen from Table 16.1 that, (1) The fix rate of Beidou single frequency ambiguity resolution is 97.9 % based on geometry mode; while for GPS, it is only 70.3 %. The success rate of Beidou is close to 100 % and only 98.66 for GPS. The main reason is that the variation of the DOP of Beidou is more smoothly than that of GPS, while for GPS, only a few satellites are useable in single epoch because the rapid variation of the satellite. (2) The ambiguity fix rate of Beidou dual frequency, triple frequency and GPS dual frequency is about the same based on geometry mode, they are all above 99 %. The success rate of Beidou dual frequency and triple frequency is 100 %, while for GPS, the ambiguity is wrongly fixed for some epochs. (3) The fix rate of ambiguity for dual system single frequency is 99.7, and the success rate is 100 %. That is much better than that of single system single frequency. (4) The fix rate of Beidou triple frequency is close to 100, but its success rate is only 95.7 % (Table 16.2).

It can be seen from the results of RTK that (1) the RMS of Beidou single frequency RTK in E, N, and U direction is about 1–3 cm, and 10 cm for that of GPS. (2) The RMS of Beidou dual frequency, triple frequency and Beidou/GPS RTK in E, N, and U are all smaller than 1 cm, and it is about 1 cm for GPS dual

Table 16.1 Statistics of ambiguity resolution for single epoch

		Fix rate	Success rate
Geometry mode	Beidou B1	97.9 %	99.99 %
		(84,610)	(84,600)
	Beidou B1/B2	99.4 %	100 %
		(85,875)	(85,875)
	Beidou B1/B2/B3	99.4 %	100 %
		(85,868)	(85,868)
	GPS L1	70.3 %	98.66 %
		(60,740)	(59,929)
	GPS L1/L2	99.8 %	~ 100 %
		(86,191)	(86,188)
	B1/L1	99.7 %	100 %
		(86157)	(86157)
	B1/B2/L1/L2	99.4 %	100 %
		(85,860)	(85,860)
Geometry-free mode	Beidou B1/B2/B3	~ 100 %	95.7 %
		(86,390)	(82,712)

Table 16.2 Results of RTK positioning for different modes (RMS, Unit: cm)

		E	N	G
Geometry mode	B1	0.97	1.65	2.75
	B1/B2	0.13	0.21	0.4
	B1/B2/B3	0.13	0.2	0.42
	GPS L1	7.42	10.9	21.5
	GPS L1/L2	0.95	0.79	1.15
	B1/L1	0.12	0.15	0.35
	B1/B2/L1/L2	0.1	0.13	0.28
Geometry-free mode	B1/B2/B3	4.03	2.64	6.31

frequency RTK; (3) The RMS of Beidou triple frequency based on geometry free mode is about 2–7 cm (Table 16.2).

All in all, the accuracy of Beidou, GPS RTK is about cm level. The success rate and reliability is related to the quality of the data, espically related to the anti-jamming ability of Beidou receiver.

16.4 Conclusions

The advantage of Beidou triple frequency signal in RTK is verified by using real data for the first time. Both the geometry and geometry-free mode are used for ambiguity resolution. The following conclusions can be get:

1. The success rate and reliability of Beidou single, dual and triple frequency ambiguity resolution is superior to that of GPS. This is because of the DOP OF GEO and IGSO varies slowly, while the ascending and descending of GPS satellite is much frequently than GPS, and this means that the ambiguity should be recalculated. At the beginning of the ascending, the elevation is low, so the quality is poor.
2. Cm level position accuracy can be achieved by geometry free based Beidou triple frequency RTK. The geometry free method is unrelated to the baseline length, and this will be useful for the application of Beidou.
3. When Beidou/GPS are combined, the position accuracy, success rateand reliability will be improved obviously, especially when the elevation angle is high or the signal is shielded.
4. The combined strategy should be developed to resolve the low reliability problem of Beidou triple frequency geometry free ambiguity resolution.
5. The measurement of GEO is seriously influenced by multi-path, the anti-jamming measures should be considered for the design of antenna and the receiver. The variation of multi-path shows systematic pattern in the long run, however, it is random in short time, its influence cannot be mitigated by RTK.

It should be noted that, only a very short baseline in Beijing are used for test and verification, more research by using mid-long baseline needs to be done in the future.

Acknowledgments This work is supported by the National Natural Science Funds of China (Grant Nos. 41020144004; 41104022), the National ''863 Program'' of China (Grant No: 2013AA122501) and the 2nd and 3rd China Satellite Navigation Conference (Grant Nos. CSNC2011-QY-13; CSNC2012-QY-3).

References

1. Guo HR, He HB, Li JL, Wang AB (2011) Estimation and mitigation of the main errors for centimetre-level compass RTK solutions over medium-long baselines. J Navig 64:S113–S126
2. Guo HR, He HB, Li JL, Wang AB (2012) Performance of triple-frequency high-precise RTK positioning with COMPASS. In: China satellite navigation conference (CSNC) 2012 proceedings, Lecture notes in electrical engineering 161, pp 371–378 doi:10.1007/978-3-642-29193-7_36
3. Yang YX, Li JL, Xu JY, Tang J, Guo HR, He HB (2011) Contribution of the compass satellite navigation system to global PNT users. Chin Sci Bull 56(26):2813–2819
4. He H (2002) Precise kinematic GPS positioning and quality control. Information Engineering University
5. Teunissen P et al (2002) A comparison of TCAR, CIR and LAMBDA GNSS ambiguity resolution. In: 15th international technical meeting of the satellite division of the institute of navigation ION GPS 2002, Portland, Oregon, USA, pp 2799–2808
6. Teunissen PJG (1995) The least-squares ambiguity decorrelation adjustment: a method for fast GPS integer ambiguity estimation. J Geodesy 70:65–82
7. Feng YM, Rizos C, Higgins M (2007) Multiple carrier ambiguity resolution and performance benefits for RTK and PPP positioning services in regional areas. In: Proceedings of ION GNSS 20th international technical meeting of the satellite division, Fort Worth, TX, USA, pp 668–678, 25–28 Sept 2007
8. Feng YM (2008) GNSS three carrier ambiguity resolution using ionosphere-reduced virtual signals. J Geodesy 82(12):847–862
9. Li BF (2008) Generation of third code and phase signals based on dual-frequency GPS measurements. In: ION GNSS 2008, Savannah, GA, USA, pp 282–283, 16–19 Sept 2008
10. Han SW (1997) Ambiguity recovery for long-range kinematic positioning. Navigation 44(2):257–290
11. Han SW, Rizos C (1999) The impact of two additional civilian GPS frequencies on ambiguity resolutions strategies. In: Proceedings of ION annual technical meeting, Cambridge, MA, pp 315–321, 28–30 June
12. Teunissen PJG, Joosten P, Tiberius CCJM (1999) Geometry-free ambiguity success rates in case of partial fixing. In: Proceedings of ION-NTM 1999, San Diego, CA, pp 201–207, 25–27 January